PCCP

Accepted Manuscript

ROYAL SOCIETY OF CHEMISTRY

www.rsc.org/pccp

Controlling the window size in mesoporous SBA-16.

L. Qin,[†] Y. Sakamoto[‡] and M.W. Anderson[*,†]

[†]Centre for Nanoporous Materials. School of Chemistry. The University of Manchester. Oxford Road. Manchester. M13 9PL. UK.

[‡]Nanoscience and Nanotechnology Research Center, Osaka Prefecture University, Sakai 599-8570, Japan

KEYWORDS SBA-16, mesoporous, minimal surface, curvature.

ABSTRACT: The structure of the mesoporous silica SBA-16 has been interrogated by careful elimination of the organic templating agent using ozone treatment. It is shown that the as-synthesised material consists of large cages connected by very narrow, ca. 7 Å, windows. These windows open up to about 20 Å following a calcination treatment that suggests that the functionality of SBA-16 could be changed markedly depending upon the post-synthesis treatment. The structure of SBA-16 is compared with surfaces of constant mean curvature. This illustrates that although most of the structure conforms to a surface of constant mean curvature the necks in the structure near the windows deviate strongly. This confirms that attractive forces in this region during synthesis play an important role in shaping the final structure. Following calcination the structure changes as the silica framework relaxes to a constant surface energy.

Introduction

Since MCM-41 was discovered[1] by Scientists in Mobil over two decades ago, ordered mesoporous materials have exhibited a huge potential for applications in many industries, such as catalysis,[2-4] adsorption,[5] separation,[6] drug delivery[7-8] and sensors.[9-11] Undoubtedly, the structures of mesoporous materials play a prominent role when evaluating their performance. Compared to interpreting the hexagonal mesoporous materials, which manly comprise hexagonally arranged, parallel[12] or twisted channels,[13] understanding cubic mesostructures is more challenging. Some contain mesocages that are connected by narrow openings,[14] while others contain interwoven channels defined by a bi-continuous interface of the inorganic moiety.[15]

A number of methods have been proposed to elucidate the cubic mesostructures. Egger et al.[16] described the cage-like mesoporous silicas by considering surfactant micelles as rigid spheres or ellipsoids, which are aggregated to form cubic unit cells. A mathematical equation has been manipulated to control the sizes of "micelles" and the distances between them to find a best model to fit the experimental structure. In another approach an intriguing relationship has been recognized between bi-continuous mesoporous silicas and infinitely periodic minimal surfaces (IPMS), on which the mean curvature H vanishes at every point.[17] Both the structures of MCM-48[18] and AMS-10[19] were found to be consistent with the G- and D-surfaces respectively. By means of high-resolution electron microscopy (HREM) and crystallography, Sakamoto et al.[20] solved the electron-density contour of the cage-like SBA-16 and reported its structure is consistent with the I-WP surface. However, this method requires a pore volume measured from the gas adsorption to refine the silica surface. Therefore, it is not possible to determine the structure for the as-synthesized mesoporous. Recently, Miyasaka et al.[21] attempted to overcome this drawback and identified the silica contour by minimizing the Helfrich energy density. The calculation neglects the unknown bending elastic module and simplified the non-uniform spontaneous curvature as a constant.

Anderson et al.[22] applied a program Surface Evolver to create minimal surfaces to model the structure of SBA-1 and a novel IPMS has been built. Based on surfaces with various void fractions, the simulated XRD patterns were calculated to compare with the experimental result and a close approximation hence could be found. Although this method can deal with the as-synthesized material filled with template, the local manipulation of the surface is not chemically reasonable since the silicate interface evolves in a uniform chemical environment and a local deviation cannot be made.

In this paper, the structure-directing agents in the as-synthesized SBA-16 have been effectively removed by ozone. This method was chosen in order to have a very gentle means to remove the template while at the same time preserving the original structural integrity of the wall structure. In this manner the structure of the ozone-treated SBA-16 is accurately characterized and compared to the as-synthesized material. The volume of mesopores exposed by ozone can hence be measured by gas sorption. On the other hand, the electron-density contours of SBA-16 are calculated based on the structure factors collected from small-angle x-ray scattering (SAXS) and the phases retrieved the HREM images which are the same as from previous reports.[23] The phases of the main Miller indices are maintained with respect to the same structure and compositions. Then the silica interfaces of both the calcined and ozone-treated SBA-16 are refined by their mesopore volumes, respectively.

Furthermore, a series of surfaces with $Im\bar{3}m$ symmetry are generated in Surface Evolver by altering the global constant mean curvature. The curvature is an indicator of the forces involved at the interface between the organic template and inorganic wall. By probing deviations from constant mean curvature it is possible to interrogate differences in this interfacial energy which in turn provide clues about the formation mechanism.

Experimental Section

Preparation of SBA-16. SBA-16 is templated by the triblock copolymer F127 (PEO_{106}-PPO_{70}-PEO_{106}), which was obtained as a gift and used as received, and co-structure directing agent hexadecyltrimethylammonium bromide C_{16}TMABr from Sigma Aldrich. In a typical preparation,[24] 1.00 g F127 and 0.12 g C_{16}TMABr were dissolved in 5.57 g concentrated HCl and 137.89 g distilled water, then 3.38 g 98% TEOS was added into the homogeneous solution at 28 °C in an oil bath and stirred for 10 mins in order to hydrolyze thoroughly. The initial crystals of SBA-16 were aged for 5 days at 90 °C under static condition. Finally the white precipitate was filtrated and dried overnight at ambient temperature.

Removal of surfactants. Calcination was performed to remove F127 templates from the as-synthesized material at 550 °C for 5 hours after a temperature ramp at 1 °C/min. Alternatively, in order to avoid the structural contraction caused by calcination and achieve higher meso-porosity, several approaches, such as solvent extraction, H_2O_2, O_3 and ultraviolet radiation, have been reported to remove the template at a temperature below 100 °C. Because of the narrow necks between the mesocages, surfactants in the as-synthesized SBA-16 are more difficult to remove compared to those in the uniform hexagonal channels in as-synthesized SBA-15. However this diffusion drawback can be neutralized by the high reactivity of F127 with oxidants, such as ozone.[25] F127 molecules in the as-synthesized material are broken down at room temperature in small fragments, which are removed from the mesopores spontaneously.

In this work, ozone flow was converted from O_2 by electric arcs in an ozone generator and introduced to the as-synthesized SBA-16 powder in a glass tray by an inverted funnel. The treatment lasted up to 96 hours to ensure a complete decomposition of F127, see Figure S1 in Supplementary Material. The suspected ozone oxidation process is shown in Figure S2 in Supplemetary Material.

Characterization.

The SAXS patterns of the SBA-16 materials were collected with a Hecus x-ray system. The specimens were loaded into sealed Borosilicate capillaries and radiated by Cu Kα from Xenocs Genix. The 2D scattered images were collected on a Dectris 100K Pilatus area detector. The 1D diffraction patterns

were then converted by Nika macro[26] in Igor Pro by means of integration along concentric circles of the images.

The HREM images were taken with a JEOL JEM-3010 microscope operating at 300kV (Cs = 1.4 mm, point resolution 0.21 nm). The samples were crushed in an agate mortar, dispersed in ethanol, and dropped on a holey carbon grid. The images were recorded with a CCD camera (ORIUS SC200D, Gatan, 2048 x 2048 pixels, pixel size 7.4 μm) at 50,000 - 80,000 times magnification under low dose conditions.

Results and discussion

Ozone-treated SBA-16. Figure 1 shows the SAXS patterns of the as-synthesized, ozone-treated and calcined SBA-16 materials. It demonstrates that in addition to maintaining the crystalline characteristics of the as-synthesized SBA-16, the deviation in the size of unit cell upon ozone treatment is negligible (< 0.5%) compared to the significant shrinkage (8.4%) resulting from calcination. The remarkable increase of the diffraction intensity on the pattern of the ozone-treated SBA-16 is expected since the removal of surfactants enhances the electron-density contrast along the crystalline silica interface of SBA-16. As seen in Figure 2, the ^{29}Si solid-state NMR spectrum of ozone-treated SBA-16 does demonstrate the condensation of Q_2 and Q_3 to Q_4, but not as much as occurs during calcination. Therefore, from the viewpoint of the unit cell size, the ozone-treated SBA-16 offers a promising representation of the inorganic framework of the as-synthesized material.

According to Figure 3, the larger hysteresis loop observed in the nitrogen adsorption isotherm of the ozone-treated SBA-16 demonstrates that the size difference between the small neck connection and large mesocages in the ozone-treated SBA-16 material is more distinct. However, the N_2 uptake of the ozone-treated SBA-16 is smaller than that of the calcined sample, which suggests a lower pore volume.

Intercepts on the vertical axis of the t-plots give the volume of micropores (Figure 4). The linear trendlines were fitted with the liquid N_2 layer thickness ranging from 0.35 to 0.45 nm, corresponding to the relative pressure from 0.25 to 0.09. It is observed that the ozone-treated SBA-16 shows a much smaller micropore volume than calcined SBA-16, as summarized in Table 1. This in turn leads to the substantial reduction in the BET surface area in the absence of these micropores. The interwall micropores are still occupied by the templates following treatment. TGA analysis shows that in the temperature range 250°C to 300°C where most of the surfactant is removed that the as-synthesised sample shows about a 15% weight loss and the ozone treated sample shows about 2 wt% loss. This indicates that most of the surfactant is removed by ozone treatment and that remaining is consistent with the template remaining in the micropores. Further corroboration of surfactant removal is given by infra-red spectroscopy, Figure S3 in Supplementary Material, which shows the loss of CH_2 stretching vibrations following treatment. It is understood that due to the diffusion obstacle, ozone predominantly reacts with the surfactants located in mesopores but has little influence on the F127 templates in the micropores of the as-synthesized SBA-16. It may well be that the presence of remaining surfactant within the micropore region protects the structure resulting in the stabilization of both the unit cell size and the Q_n ratios.

Structure reconstruction. The electron density maps of ozone-treated and calcined SBA-16 materials are derived from the structure factors |F(hkl)| collected from SAXS and the reported phases[23] based on a concise equation for space group $Im\bar{3}m$ in the International Table for X-ray Diffraction, (1952 edition).[29]

$$\rho(xyz) = \frac{8}{V} \sum_{hkl} F(hkl)\ \cos 2\pi hx \cos 2\pi ky \cos 2\pi lz$$

Statistically in a powder SAXS pattern, Miller indices, which are equivalent with arbitrary orientation, make an equal contribution to a single diffraction peak. As a consequence, the intensity of a diffraction peak is divided by the multiplicities of the specific *hkl* and |F(hkl)| is proportional to the square root of the quotient, as summarized in Table 2.

Once the electron-density map is constructed, sample points are spread out evenly in a unit cell which contains both silica and mesopore regions. The electron densities of individual points are calculated according to the equation above. The mesopore volume proportion, which is derived from the gas sorption, is applied to select the points located in the mesopore region and further distinguish the electron-density threshold of the silica interface (Table3). A 3D plot of the SBA-16 mesostructure can hence be presented by using a less-than-or-equal-to inequality with the concise expression and the threshold. Only the first six peaks are selected for the fit, which play the major role in the structure reconstruction and suffice to represent the contour of the SBA-16 silica wall. As seen in Figure 5, the neck connection between mesocages in the ozone-treated SBA-16 is much narrower than that in the calcined material.

Validity of using the reported phases. It sounds questionable to rebuild the silica structure of a centain SBA-16 sample by using the reported phase information. Therefore the structures of the calcined and ozone-treated SBA-16 were determined by HREM. As observed in Figure 6, both of the two materials show the satisfying regularity in the $Im\bar{3}m$ structure along all three directions and the diffraction phases can be determined.

Simulation of constant mean-curvature surfaces. The IPMS was generated in Surface Evolver, written by Brakke.[30] Surface Evolver treats a surface as a union of simplified small triangles, which collectively constitute a reasonable approximation to a smooth surface. The minimization of the area of the triangles will eventually lead to the minimal surface. The data file for the surface of SBA-16 materials is based on the one written for I-WP (space group $Im\bar{3}m$) minimal surface, which is available on Brakke's webpage.[31] The parameter *h_zero*, which controls the global mean curvature of the surface in Surface Evolver, is adjusted gradually in order to obtain a void volume proportion which is consistent with the mesopore fraction obtained from the gas sorption analyses of ozone-treated and calcined SBA-16 materials respectively (Table 3).

The resultant constant mean curvature surface is compared to the electron density map of the SBA-16 mesostructure. With the purpose of illustrating a comparison of the interior unit cell, the 3D space is sliced into a group of discrete 2D layers.

Deviation at the neck connections of the ozone-treated SBA-16. Only one pair of the 2D slice comparison between the calculated silica interfaces of the calcined and ozone-treated SBA-16 and their corresponding simulated constant mean curvature surfaces are shown in Figure 7. More figures are shown in the supporting information. A noticeable deviation at the neck connections is observed on the comparison image of the ozone-treated SBA-16. The silica wall does not follow the constant mean curvature surface. On the other hand, on the comparison image of the calcined SBA-16, an excellent match has been found between the silica wall and the simulated surface. However, the silica wall in other regions of the unit cell, away from the neck regions, of the ozone-treated SBA-16 also form a constant mean curvature surface.

Therefore, it is conjectured that there is an attractive affiliation between components located in the window connection and the siliceous moiety, which resists the inorganic interface reducing its surface energy to form the constant mean curvature surface. When the templates of the as-synthesized material are removed by calcination, the affiliation on the silica wall is released and the surface is able to minimize its surface energy at the high temperature to form a constant mean curvature surface, as shown in Figure 7 left. Because the neck connection is too narrow to accommodate the surfactant templates it is reasonable to postulate that the neck connections are filled with water containing Cl^- which provides this affiliation to the silica wall.

These results offer an interesting possibility to control the window size in SBA-16 in the important range between 7 Å and 20 Å. By first removing the template via ozone treatment it may well be possible to open up the pores in a predictable manner by careful calcination. Certain properties of SBA-16 are likely to change dramatically between a sample with 7 Å windows and one with 20 Å windows. This also offers a potential method to control structure of other mesoporous phases, in particular the cage-like structures through a post synthesis treatment.

Conclusion

Surfactants in the mesopores of the as-synthesized SBA-16 are effectively removed by ozone leaving the parts embedded within the micropores unaffected. The ozone-treated SBA-16 maintains the size of unit cell and the mesostructure of the as-synthesized material. The narrower neck connections between mesocages of the ozone-treated SBA-16 compared to the calcined material, 7Å versus 20 Å, shows the potential application in catalysis and separation where the diffusion characteristics of the material can be controlled through control of the window neck size.

Combining the amplitudes of structure factors calculated from the SAXS pattern with the known phases of reflections permits the easy generation of electron-density maps of SBA-16 with acceptable accuracy. By applying the mesopore fraction obtaned from gas sorption analysis as a reference, the mesostructure of the as-synthesized SBA-16, represented by that of the ozone-treated material, was determined. The discrepancy between the as-synthesized SBA-16 silica wall and the simulated constant mean curvature surface at the neck connections indicates that an attractive affiliation resists the silica wall reducing its surface energy in this region. Such interactions are crucial in the formation of the resulting structure of SBA-16 and may well operate for other mesoporous materials, especially those with cage structures syntheised from block co-polymers where part of the template remains embedded in the silica wall. Calcination acts to reform the mesoporous structure allowing the surface energy free to minimize, forming a constant mean curvature surface.

ASSOCIATED CONTENT

Supporting Information. The supporting information includes: (i) a series of comparisons between electron density contours and constant mean curvature surfaces for both calcined and ozone treated SBA-16; (ii) constant mean curvature surface for calcined SBA-16 calculated with *Surface Evolver*; (iii) the datafile for input to *Surface Evolver* in order to calculate the constant mean curvature surface related to calcined SBA-16; (iv) Mathematica code for the calculation of iso-electron density contour of calcined SBA-16; (v) Mathematica code for comparison of electron density maps with surface of constant mean curvature. This material is available free of charge via the Internet at http://pubs.acs.org.

AUTHOR INFORMATION

Corresponding Author

* m.anderson@manchester.ac.uk

Author Contributions

The manuscript was written through contributions of all authors. / All authors have given approval to the final version of the manuscript. / †‡These authors contributed equally.

Funding Sources

China Scholarship Council and The University of Manchester

ACKNOWLEDGMENT

The authors would like to thank China Scholarship Council and The University of Manchester for financial support to LQ. We also thank Ken Brakke for useful discussions concerning the use of *Surface Evolver*.

REFERENCES

(1) Beck, J. S.; Vartuli, J. C.; Roth, W. J.; Leonowicz, M. E.; Kresge, C. T.; Schmitt, K. D.; Chu, C. T. W.; Olson, D. H.; Sheppard, E. W.; McCullen, S. B.; Higgins, J. B.; Schlenker, J. L. *J. Am. Chem. Soc.* **1992,** *114*, 10834.

(2) Beck, J. S.; Socha, R. F.; Shihabi, D. S.; Vartuli, J. C. Selective Catalytic Reduction (SCR) of Nitrogen Oxides. US5143707, September 1, 1992.

(3) Borghard, W. S.; Chu, C. T.; Degnan, T. F.; Shih, S. S. Aromatics Saturation With Catalysts Comprising Crystalline Ultra-Large Pore Oxide Materials. US5264641, November 23, 1993.
(4) Kresge, C. T.; Marler, D. O.; Rav, G. S.; Rose, B. H. Supported Heteropoly Acid Catalysts. US5366945, November 22, 1994.
(5) Ioneva, M. A.; Newman, G. K.; Harwell, J. H. *AIChE Symp. Ser.* **1995,** *309*, 40.
(6) Grun, M.; Kurganov, A. A.; Schacht, S.; Schuth, F.; Unger, K. K. *J. Chromatogr., A* **1996,** *740*, 1.
(7) Hartmann, M. *Chem. Mater.* **2005,** *17*, 4577.
(8) Radu, D. R. Mesoporous Silica Nanomaterials for Applications in Catalysis, Sensing, Drug Delivery and Gene Transfection. Ph.D. Dissertation, Iowa State University, Ames, IA, 2004.
(9) Oh, H.; Kim, J. H.; Jang, J. *J. Mater. Chem.* **2012,** *22*, 21828.
(10) Wu, C.-G.; Bein, T. *Chem. Mater.* **1994,** *6*, 1109.
(11) Leon, R.; Margolese, D.; Stucky, G.; Petroff, P. M. *Phys. Rev. B: Condens. Matter Mater. Phys.* **1995,** *52*, R2285.
(12) Kruk, M.; Jaroniec, M.; Ko, C. H.; Ryoo, R. *Chem. Mat.* **2000,** *12*, 1961.
(13) Qiu, H.; Inoue, Y.; Che, S. *Angew. Chem., Int. Ed.* **2009,** *48*, 3069.
(14) Anderson, M. W.; Ohsuna, T.; Sakamoto, Y.; Liu, Z.; Carlsson, A.; Terasaki, O. *Chem. Commun. (Cambridge, U. K.)* **2004**, 907.
(15) Alfredsson, V.; Anderson, M. W. *Chem. Mater.* **1996,** *8*, 1141.
(16) Egger, C. C.; Anderson, M. W.; Tiddy, G. J. T.; Casci, J. L. *Physical Chemistry Chemical Physics* **2005,** *7*, 1845.
(17) Hyde, S.; Blum, Z.; Landh, T.; Lidin, S.; Ninham, B. W.; Andersson, S.; Larsson, K., *The Language of Shape: The Role of Curvature in Condensed Matter: Physics, Chemistry and Biology*; Elsevier Science: Amsterdam, 1996.
(18) Huo, Q. S.; Leon, R.; Petroff, P. M.; Stucky, G. D. *Science* **1995,** *268*, 1324.
(19) Gao, C. B.; Sakamoto, Y.; Sakamoto, K.; Terasaki, O.; Che, S. N. *Angew. Chem., Int. Ed.* **2006,** *45*, 4295.
(20) Sakamoto, Y.; Kaneda, M.; Terasaki, O.; Zhao, D. Y.; Kim, J. M.; Stucky, G.; Shim, H. J.; Ryoo, R. *Nature* **2000,** *408*, 449.
(21) Miyasaka, K.; Garcia Bennett, A.; Han, L.; Han, Y.; Xiao, C.; Fujita, N.; Castle, T.; Sakamoto, Y.; Che, S.; Terasaki, O. *Interface Focus* **2012,** *2*, 634.
(22) Anderson, M. W.; Egger, C. C.; Tiddy, G. J. T.; Casci, J. L.; Brakke, K. A. *Angew. Chem., Int. Ed.* **2005,** *44*, 3243.
(23) Hughes, P. J. The Synthesis, Characterization and Modelling of Nanostructured Materials and their Application as Catalysts Supports. Ph.D. Dissertation, The University of Manchester, Manchester, U.K., 2005.
(24) Mesa, M.; Sierra, L.; Patarin, J.; Guth, J. L. *Solid State Sciences* **2005,** *7*, 990.
(25) Xie, L. L.; Li, Q. H.; Yuan, H.; Wang, L. J.; Tian, Z.; Bing, N. C. *Acta Chim. Sin. (Engl. Ed.)* **2008,** *66*, 2113.
(26) Ilavsky, J. *Journal of Applied Crystallography* **2012,** *45*, 324.
(27) Wang, X.; Cheng, S.; Chan, J. C. C.; Chao, J. C. H. *Microporous Mesoporous Mater.* **2006,** *96*, 321.
(28) Gobin, O. C.; Wan, Y.; Zhao, D. Y.; Kleitz, F.; Kaliaguine, S. *J. Phys. Chem. C* **2007,** *111*, 3053.
(29) *International Tables for X-Ray Crystallography, Volume 1*, Henry, N. F. M.; Lonsdale, K., Eds. Kynock Press: Birmingham, U.K., 1952.
(30) Brakke, K. A. *Exp. Math.* **1992,** *1*, 141.
(31) I-WP surface. http://www.susqu.edu/brakke/evolver/downloads/s14adj.fe (accessed Jun 18, 2013),

Table 1. Summary of the pore size information of the calcined and ozone-treated SBA-16. The mesopore proportion is calculated based on the reported density of silica ρ = 2.2 g cm^{-3}, which is measured by Helium pycnometry.[28]

	Calcined SBA-16	Ozone-treated SBA-16
BET surface area / m^2 g^{-1}	663.80	430.13
Total pore volume / cm^3 g^{-1}	0.4488	0.3678
Micropore volume / cm^3 g^{-1}	0.1083	0.0089
Mesopore volume / cm^3 g^{-1}	0.3405	0.3589
Mesopore proportion	0.3768	0.3853

Table 2. experimental structure factors and reported phases of the first *hkl*s of the calcined and ozone-treated SBA-16.

h	k	l	Calcined SBA-16			Ozone-treated SBA-16		
			d-spacing / Å	phase	$\|F(hkl)\|$	d-spacing / Å	phase	$\|F(hkl)\|$
1	1	0	98.1	0	100.00	106.6	0	100.00
2	0	0	69.4	0	19.23	75.4	0	20.24
2	1	1	56.7	0	1.84	61.6	0	1.06
2	2	0	49.1	0	14.09	53.3	0	7.84

Table 3. electron-density contours of the calcined and ozone-treated SBA-16 and the constant mean curvatures of the corresponding surfaces.

	Calcined SBA-16	Ozone-treated SBA-16
Electron density threshold	-1.444	-3.984
Real mean curvature of silica surface / Å^{-}	0.00978	0.00830

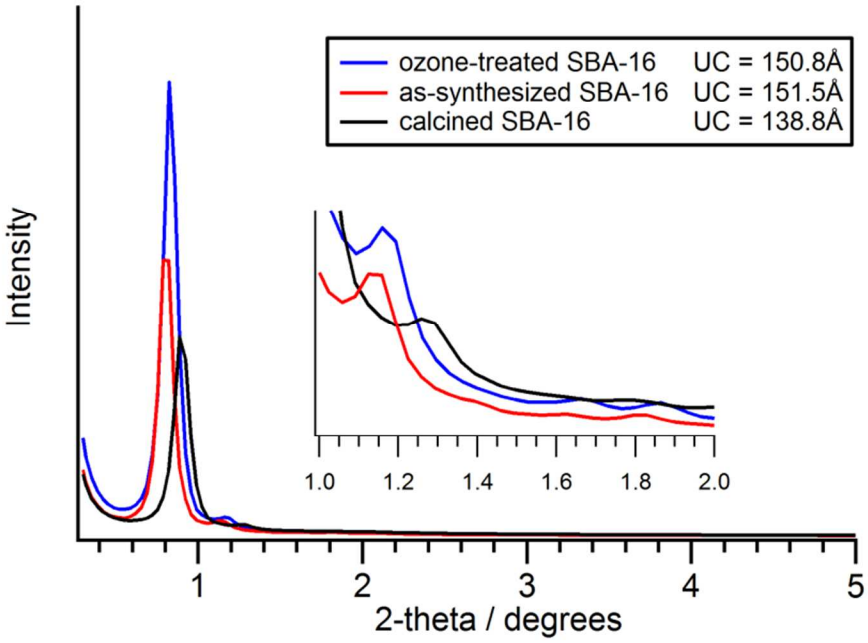

Figure 1. SAXS patterns of the calcined (black), as-synthesized (red) and ozone-treated (blue) SBA-16. Inset is the magnified patterns ranging from 1.0 to 2.0 degrees of 2-theta. The sizes of unit cells of the three materials are listed alonside the corresponding figure legends.

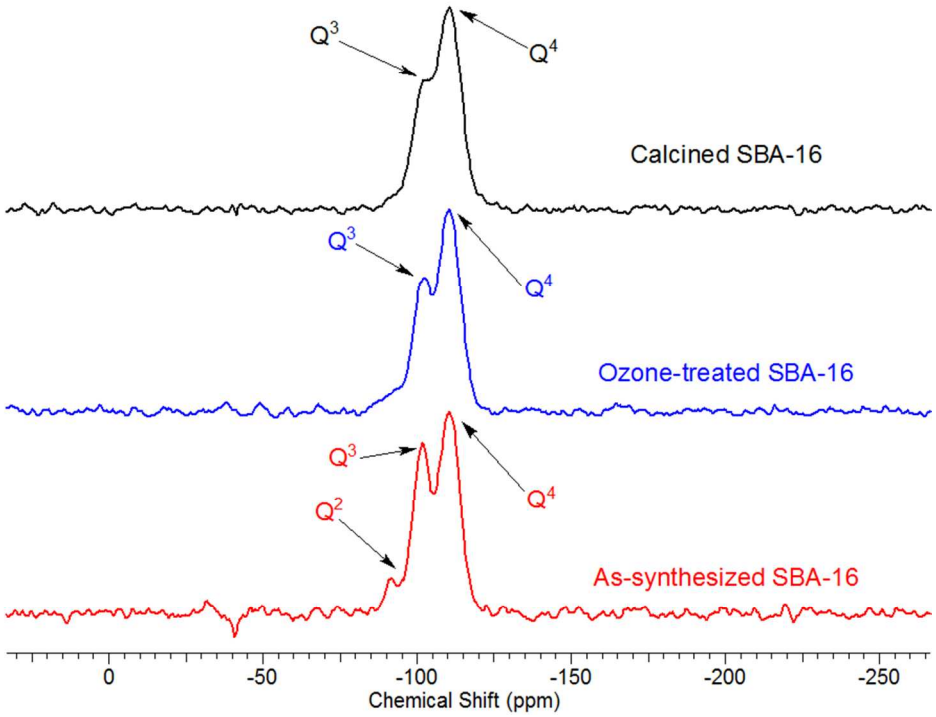

Figure 2. ^{29}Si solid-state NMR spectra of the calcined (black), ozone-treated (blue) and as-synthesized (red) SBA-16. The chemical shifts of Q_2, Q_3 and Q_4 are -92, -103 and -110 ppm, respectively.[27]

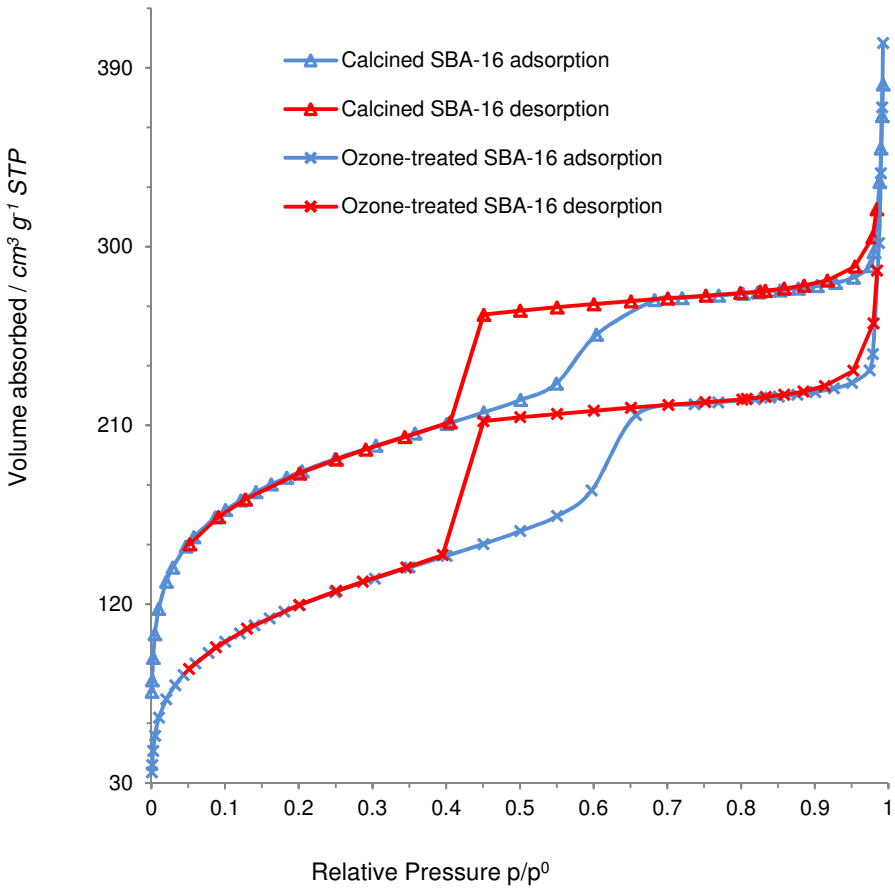

Figure 3. N_2 sorption isotherms of the calcined (triangle) and ozone-treated (cross) SBA-16. Both of the adsorption branches are in blue and desorption branches in red.

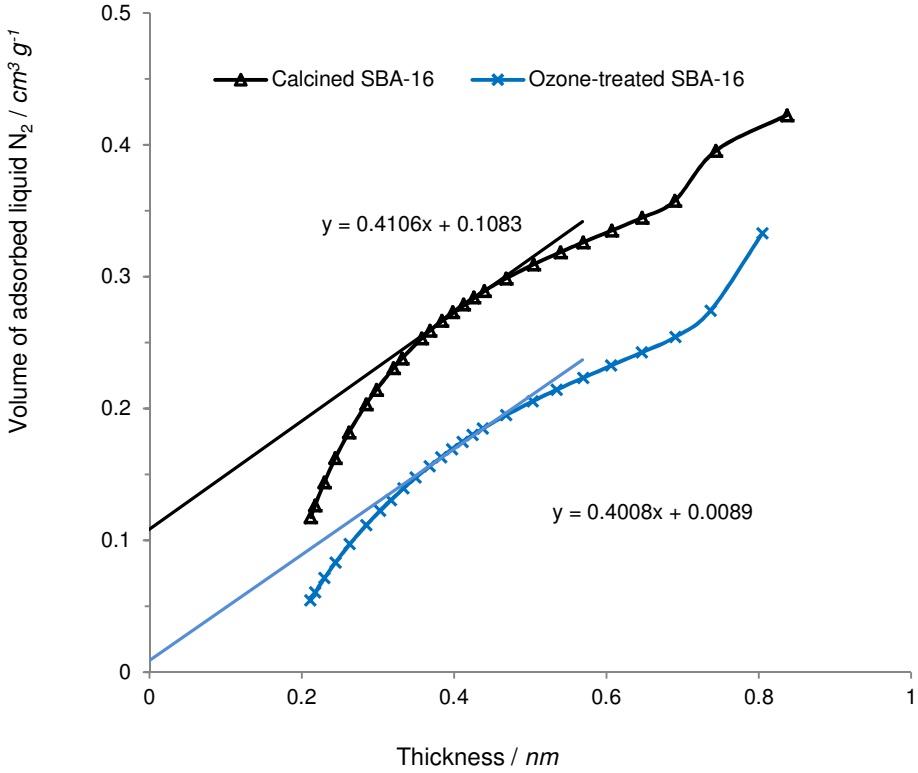

Figure 4. t-plots of the calcined (triangle, black) and ozone-treated (cross, blue) SBA-16.

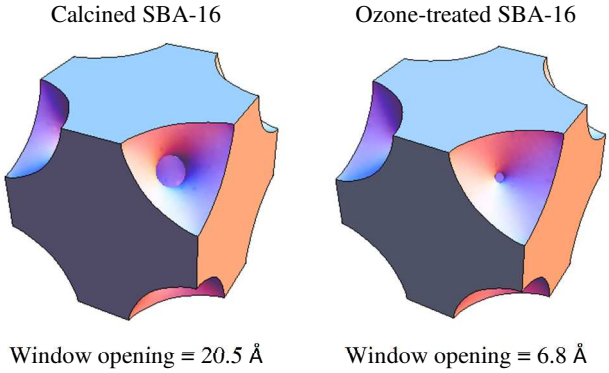

Figure 5. 3D plots of the calcined (left) and ozone-treated (right) SBA-16 with sizes of window openings.

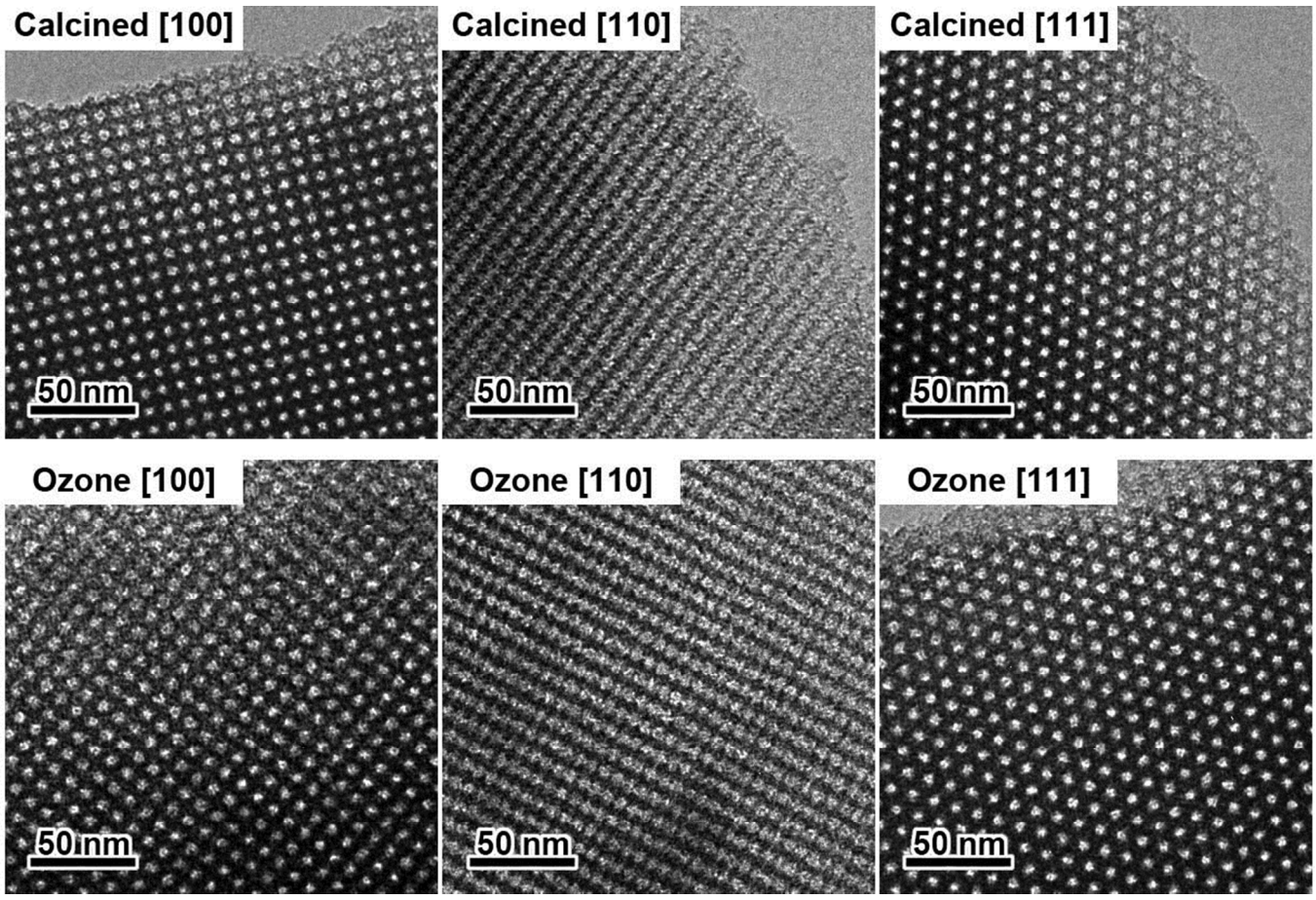

Figure 6. HREM images of the calcined (top) and ozone-treated (bottom) SBA-16 along [100], [110] and [111] directions.

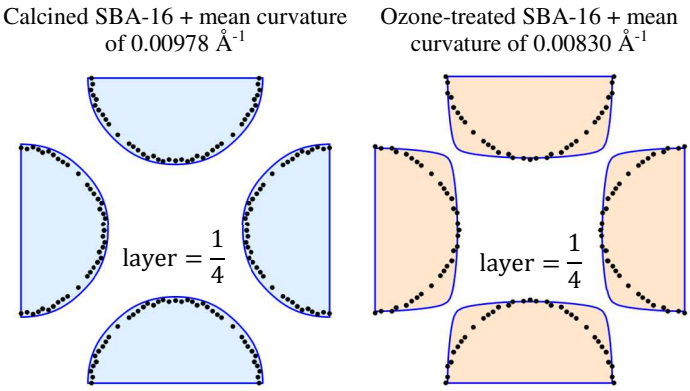

Figure 7. 2D comparison layer between the electron-density contours of the calcined (left, colored region) and ozone-treated (right, colored region) SBA-16 and their matching constant mean curvature surfaces (dotted lines in both images).

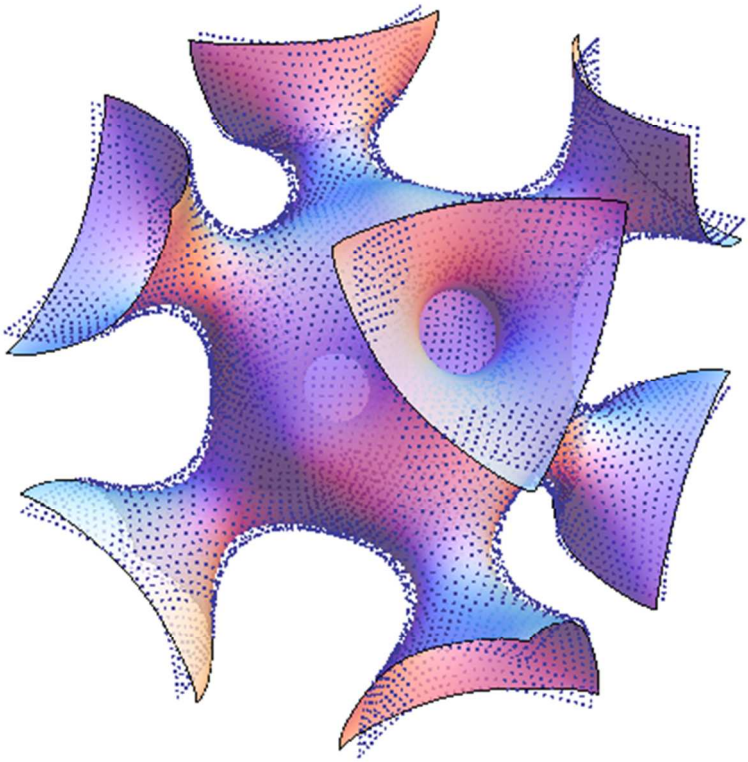

TOC: Dotted line: constant mean curvature with $Im\bar{3}m$ symmetry. Solid surface: electron density map of calcined SBA-16.